Eur. Phys. J. D **3**, 119–122 (1998)

THE EUROPEAN PHYSICAL JOURNAL D

Measurement of the Barkas effect in hydrogen

R. Schmidt[1,a], H. Daniel[1], F.J. Hartmann[1], P. Hauser[2], F. Kottmann[3], M. Mühlbauer[1], C. Petitjean[2], W. Schott[1], D. Taqqu[2], and P. Wojciechowski[1]

[1] Physik-Department, Technische Universität München, 85747 Garching, Germany
[2] Paul Scherrer Institut, 5232 Villigen PSI, Switzerland
[3] Institut für Hochenergiephysik, ETH Zürich, 8093 Zürich, Switzerland

Received: 23 April 1998 / Accepted: 7 May 1998

Abstract. The stopping power of gaseous hydrogen for positive and negative muons at energies ranging from 3 to 100 keV has been measured by time-of-flight. A pronounced Barkas effect was observed: the energy loss in hydrogen for negative muons was found to be significantly smaller than that for positive muons.

PACS. 34.50.Bw Energy loss and stopping power

1 Introduction

In 1956 Barkas and coworkers [1] found a difference between the low-energy stopping power for negative and positive pions. This effect comes about by the polarizing influence of low-energy charged particles on the electron distribution in matter. At velocities around the Bohr velocity the electron distribution is no longer static as it has been assumed by Bethe and Bloch [2,3]. The density of the electrons seen by the particle rises for positive and is diminished for negative particles.

To include this effect, the formula for the stopping power S can be expanded to higher powers of the particle charge z:

$$S = \frac{S_0}{v^2}(L_0 z^2 + L_1 z^3 + L_2 z^4) \tag{1}$$

with

$$S_0 = \frac{N_A e^4}{4\pi\epsilon_0 m_e}\frac{Z}{A}; \tag{2}$$

here N_A is the Avogadro constant, e the elementary charge, ϵ_0 the electric constant, m_e the electron mass, v the particle velocity, and Z and A are the atomic and mass numbers of the target material, respectively. Whereas $L_0 z^2$, the Bethe term, and $L_2 z^4$, the Bloch term, are independent of the sign of the particle charge, $L_1 z^3$, the Barkas term, has a different sign for positive and negative particles.

From the stopping powers S_+ and S_- for positive and negative particles, respectively, the factor $\dfrac{(S_+ - S_-)}{(S_+ + S_-)}$ may be derived for quantifying the Barkas effect. According to equation (1) it is given by

$$\frac{S_+ - S_-}{S_+ + S_-} = \frac{L_1}{L_0 + L_2}\,. \tag{3}$$

After the first observation of Barkas *et al.*, measurements with Σ-particles [4] and with slow pions in hydrogen were performed [5]. Later on the Barkas effect was explored with muons in aluminum and copper [6].

Experimental data on the stopping power for negative particles heavier than electrons are scarce: Medenwaldt *et al.* measured the stopping power for antiprotons of silicon and gold [7–9] and the OBELIX collaboration at CERN that of hydrogen [10–12]. At Paul Scherrer Institut (PSI) the stopping power of hydrogen for negative muons was determined [13]. Recently experiments with negative muons of low energies were performed with gold and MgF_2 [14], and with kapton [15], the latter down to 1 eV. As the electronic stopping power depends only on the velocity of the particles the muon and pion results can be compared with the proton and antiproton stopping power data at the same velocity; this is so because at the investigated energies the so-called nuclear contributions to the stopping power are small.

A comparison of different calculations of the proton stopping power of hydrogen with the data collected in reference [16] shows good agreement with a distorted-wave Born approximation (DWBA) calculation and a coupled-channel atomic-orbital (AO) calculation [17]. For negative particles an adiabatic-ionization calculation deviates strongly from the DWBA and AO calculations and from $\bar{p}$ and μ^- experimental results which themselves do not agree well with each other. The situation is complicated by the molecular binding of the experimental targets whose effect is to increase S considerably [18]. Recently

[a] e-mail: rolf@e18.physik.tu-muenchen.de

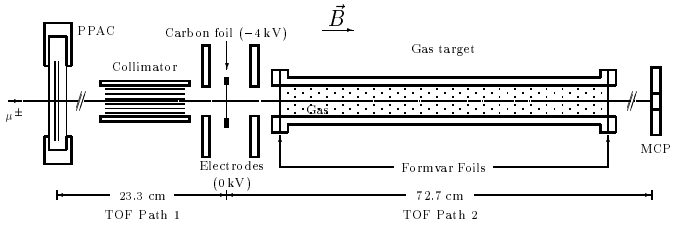

Fig. 1. Experimental set up of the time-of-flight sections inside the superconducting solenoid; PPAC: parallel plate avalanche counter, MCP: microchannel plate detector.

the Barkas effect measured by Wilhelm *et al.* [6] was quantitatively reproduced by a plasma calculation [19].

The advantage of the time-of-flight (TOF) technique as used in our experiment at PSI is that the same arrangement can be used for positive and negative muons simply by changing the polarity of the magnets in the muon beam line. Furthermore the TOF method leads to a direct determination of the muon energy by using simple laws of mechanics and electrodynamics. The TOF set up employed in the present experiment was already used for solid targets by Wojciechowski *et al.* [20]. The stopping power for *positive* muons could be measured down to an energy of the muons entering the target gas of about 6 keV, in the case of *negative* muons even down to 3 keV. The energy limit is higher for positive muons mainly due to muonium formation inside the target material.

2 Experimental set up

Details of our experimental methods with two TOF sections are given in reference [20]. The set up is shown in Figure 1. A parallel–plate avalanche counter (PPAC) gives a signal when a muon enters the first TOF section. At the end of the first section, which is immediately followed by the second one, a thin carbon foil of $3\,\mu g/cm^2$ is placed to provide the information on the time when the muon passes (*cf.* below). A microchannel plate detector (MCP) at the end of the second section provides the stop signal for the second TOF measurement.

In the carbon foil the muon knocks out electrons. These electrons are accelerated in a constant electric field around the foil towards the MCP. This field is generated by putting the carbon foil on a negative voltage of −4 kV and limited by two electrodes, one in front of the foil and one behind it, both at earth potential (0 keV). The TOF of the electrons and the time of their stop in the MCP give the additional information necessary to determine the two TOFs of the muon. A direct measurement of the muon travel time between the two sections (*cf.* Fig. 1) with a counter is not possible, because the energy loss in the counter would be too high compared with that in the gas.

The experiment was performed in the πE5 area of Paul Scherrer Institut with muons of about 10 MeV/c incoming momentum. Mylar foils with a thickness of $16\,\mu m$ and the PPAC decelerated the muons by such an amount that the flux of muons with energies below 100 keV was maximal; this resulted in a wide energy spectrum down to a few keV. The whole TOF set up was placed inside a superconducting solenoid generating a field of 3 T parallel to the beam axis, keeping the muons gyrating along the field lines. Muons moving at too large an angle to the axis would have been registered with too small energy. To remove these muons a collimator with 3 mm spacing, which limited the divergence of the muon beam, was placed in front of the carbon foil.

The gas target, an aluminum tube 209 mm long and 20 mm in diameter, and with front and rear windows of $5\,\mu g/cm^2$ formvar each, was placed in the second section, 34 mm behind the carbon foil and outside the accelerating field. The target windows could withstand a pressure inside the target of more than 60 hPa, the maximum pressure used in the measurements with hydrogen. This pressure is equivalent to $1.1\,\mu g/cm^2$ of hydrogen inside the target which leads to roughly the same energy loss as $5\,\mu g/cm^2$ carbon. The gas was kept flowing through the target to avoid contamination, and a pressure-regulating system ensured that the pressure was held at the desired value.

3 Data analysis

For the determination of the two TOFs the time when the muon leaves the first and enters the second TOF section has to be known. This time could not be measured directly. With Δt_e being the TOF of the secondary electrons from the carbon foil to the MCP, the first and second TOFs Δt_1^μ and Δt_2^μ, respectively, of the muons are

$$\begin{aligned} \Delta t_1^\mu &= t_{MCP}^e - \Delta t_e - t_{PPAC}, \\ \Delta t_2^\mu &= t_{MCP}^\mu - t_{MCP}^e + \Delta t_e \end{aligned} \tag{4}$$

where t_{MCP}^e is the time when the electrons reach the MCP, and t_{PPAC} and t_{MCP}^μ, respectively, are the times when the muon hits the PPAC and the MCP.

As the stopping power for electrons at the energies used in this experiment is not known with sufficient precision, Δt_e was determined from the times measured at relatively high muon energies around 120 keV. At these energies the stopping power is low (about 20% of the stopping power at the Bragg maximum). The Bethe–Bloch formula is valid and thus the stopping power data for protons of the same velocity, as published by Janni [22], are a good approximation for the stopping power of positive and negative muons. Furthermore at these muon energies Δt_e has a large influence on the measured TOFs allowing a rather accurate determination of Δt_e:

$$\Delta t_e = t_{MCP}^e - t_{MCP}^\mu + \Delta t_{\mu c}. \tag{5}$$

The muon TOF $\Delta t_{\mu c}$ was calculated from the energy of the incoming muon, the Janni data and the geometry of the TOF sections.

To derive the stopping power in the gas with our set up we first made measurements with the carbon foil only,

then with the gas target filled with 10 hPa of hydrogen (to prevent the formvar windows from charging and to flush impurities out of the target). Finally the gas measurements were performed with hydrogen at 60 hPa, each measurement with positive and negative muons. Energy and stopping power of the muons in the carbon foil could then easily be determined from the TOF data of the measurement without gas target (*cf.* Ref. [20]).

In order to determine the stopping power of the target windows, two sets of data, one with the almost empty target (10 hPa H_2) and one with the filled target (60 hPa H_2), were needed.

While the evaluation of the muon energy T_1 in front of the carbon foil from Δt_1^μ is still the same as in reference [20], the determination of the muon energy T_2 behind the gas target is more difficult. Now Δt_2^μ is the sum of the TOF values Δt_f^μ, Δt_t^μ, and Δt_b^μ for the sections in front of, inside, and behind the gas target, respectively,

$$\Delta t_2^\mu = \Delta t_f^\mu + \Delta t_t^\mu + \Delta t_b^\mu \tag{6}$$

with each time Δt_i^μ, $i = f, t, b$, given by

$$\Delta t_i^\mu = \int_{section\ i} \sqrt{\frac{m_\mu}{2T_\mu(x)}} dx. \tag{7}$$

The kinetic energy of the muon behind the target is

$$T_2 = T_1 - \Delta T_C - \Delta T_W - \Delta T_{gas} - \Delta T'_W \tag{8}$$

with the energy losses ΔT_C, ΔT_W, $\Delta T'_W$, and ΔT_{gas} in the carbon foil, in the front and rear windows, and in the gas, respectively. Each ΔT is a function of the muon energy at the location where the energy loss takes place. From the combination of equations (6) through (8) for all energies in the observed energy region, the energy-loss data for the windows and the gas were derived. From this the stopping power S in the gas was determined. The minimum muon energy in the gas, at which we could measure, was limited by the total energy loss. A higher gas pressure gives more precise results but increases at the same time the minimum energy accessible with our experiment.

4 4 Results and discussion

The analysis led to the stopping–power data shown in Figure 2. The horizontal bars show the regions of muon energies which contribute to the corresponding data points. The Barkas effect in hydrogen is clearly observed. At low energies the values for μ^- are significantly smaller than for μ^+.

To parametrize the data the stopping power formula introduced by Varelas and Biersack was taken [21]:

$$S = S_H S_L / (S_H + S_L) \tag{9}$$

with

$$S_L = a_1(\gamma T)^{a_2},$$
$$S_H = \frac{a_3}{\gamma T} \ln\left(\frac{a_4}{\gamma T} + a_5 \gamma T + 1\right) \tag{10}$$

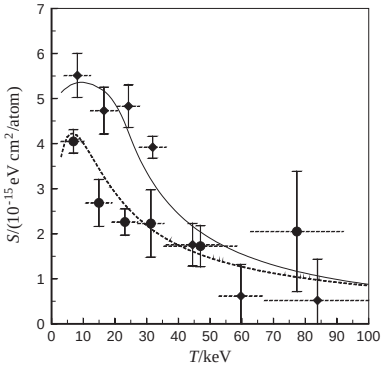

Fig. 2. Stopping power of hydrogen for positive and negative muons. Diamonds and solid line: μ^+ data; full circles and dashed line: μ^- data. Horizontal bars: energy interval of the muons taken for the respective data point. The lines are best fits according to equation (9), for μ^+ corrected for muonium formation.

Table 1. Parameter values found in this experiment for the Varelas–Biersack stopping power function [21] for hydrogen.

particle	a_1	a_2	a_3	$a_4/10^3$	a_5
μ^+	> 10	0.45	116±19	565±166	0.1159
μ^-	0.94±0.06	0.45	165±14	12±7	0.1159

(S in eV cm^2/(10^{15} atoms) and T in keV). γ is the ratio of the proton mass to the particle mass.

The parameters from the best fit of the stopping power S_{μ^-} of μ^- are shown in Table 1. The parameters $a_2 = 0.45$ and $a_5 = 0.1159$ were taken from reference [16] as they influence S only very weakly in the investigated energy region between 3 keV and 100 keV. In order to reproduce the high–energy part of the stopping–power function at an energy of 120 keV, S_{μ^-}(120 keV) was set to be equal to the proton stopping power at $\gamma\times$120 keV (*cf.* Fig. 2).

For μ^+ muonium formation becomes important for energies below 20 keV. The muonium formation was considered with an effective charge z^* taken from the corresponding proton values from reference [22]. Corrections up to z^3 according to equation (1) were taken into account. The effective charge of the muonium was taken to be zero. The fit to these corrected stopping power values is also shown in Figure 2. For $a_1 > 10$ the stopping power for the measured μ^+ with an energy larger than 6 keV is determined only by the high energy part S_H.

In Figure 3 the stopping power data are compared with other measurements with negative muons [13], with the antiproton stopping power from reference [11] and the proton data compiled by Janni [22]. More recent measurements of the hydrogen stopping power for protons with energies below 20 keV [23] agree fairly well with these data.

While the maximum value of the stopping power we found for μ^+ is smaller than that for protons, our measurements for μ^- brought about higher values than those given for antiprotons [11] and for μ^- in reference [13]. Our higher maximum value of the μ^- stopping–power,

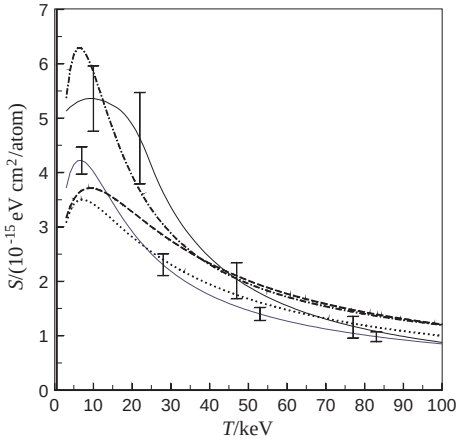

Fig. 3. Best fit to the stopping power of hydrogen for μ^+ (upper solid line) and μ^- (lower solid line). For four energies error bars of the fit are plotted. Dot-dashed line: proton data for hydrogen taken from reference [22]; dashed line: antiproton data taken from reference [11]; dotted line: μ^- data taken from reference [13]. The proton and antiproton data have been rescaled according to $T_{p,\bar{p}} = \gamma T_\mu$ with $\gamma = m_p/m_\mu = 8.85$.

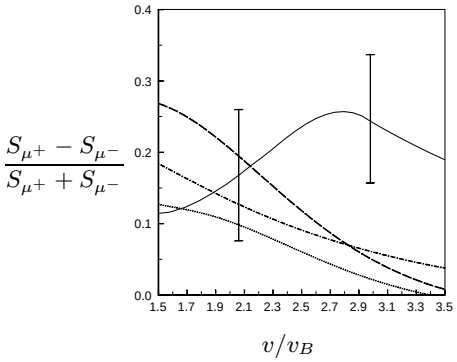

Fig. 4. $(S_{\mu^+} - S_{\mu^-})/(S_{\mu^+} + S_{\mu^-})$ as a function of v/v_B, with $v/v_B = 0.596\sqrt{E/\mathrm{keV}}$. Only for two points the error bars are plotted. Solid line: data from this experiment; dashed line: data from a comparison of proton [22] and antiproton [11] results; dot-dashed line: oscillator model calculations [25]; dotted line: distorted-wave Born approximation [17,18].

however, is in agreement with calculations by Cohen using the classical trajectory Monte–Carlo method [24].

The quantity $(S_{\mu^+} - S_{\mu^-})/(S_{\mu^+} + S_{\mu^-})$ is plotted in Figure 4 as a function of v/v_B, where v_B is the Bohr velocity. The muon data are compared with those derived from the difference of proton [22] and antiproton [11] results, and with calculations for the proton stopping power based on the oscillator model [25] and the distorted-wave Born approximation [17,18].

While the different sets of data agree for velocities around the Bohr velocity, for $v \approx 3v_B$ the measured Barkas term is higher than that for protons and antiprotons and that predicted by the calculations with the oscillator model and the DWBA.

We thank the accelerator team of Paul Scherrer Institut for providing the intense, high-quality muon beam and H. Angerer, M. Aigner, and H. Grünwald of Technische Universität München for their technical assistance. We appreciate the production of the formvar windows for the gas target by B. Leoni and of the carbon foils by Katharina Nacke and Dr. P. Maier-Komor. Financial support by the German Bundesministerium für Bildung, Wissenschaft, Forschung und Technologie and by the Beschleunigerlaboratorium der Universität und der Technischen Universität München is acknowledged.

References

1. W.H. Barkas, W. Birnbaum, F.M. Smith, Phys. Rev. **101**, 778 (1956).
2. H. Bethe, Ann. Phys. **5**, 325 (1930).
3. F. Bloch, Ann. Phys. **16**, 287 (1933).
4. W.H. Barkas, J.N. Dyer, H.H. Heckman, Phys. Rev. Lett. **11**, 26 (1963).
5. H.H. Heckman, P.J. Lindstrom, Phys. Rev. Lett. **22**, 871 (1969).
6. W. Wilhelm, H. Daniel, F.J. Hartmann, Phys. Lett. **98B**, 33 (1981).
7. R. Medenwaldt, S.P. Møller, E. Uggerhøj, T. Worm, P. Hvelplund, H. Knudsen, K. Elsener, E. Morenzoni, Nucl. Instr. Methods B **58**, 1 (1991).
8. R. Medenwaldt, S.P. Møller, E. Uggerhøj, T. Worm, P. Hvelplund, H. Knudsen, K. Elsener, E. Morenzoni, Physics Letters A **155**, 155 (1991).
9. S.P. Møller, E. Uggerhøj, H. Bluhme, H. Knudsen, U. Mikkelsen, K. Paludan, E. Morenzoni, Nucl. Instr. Methods B **122**, 162 (1997).
10. OBELIX Collaboration, A. Adamo *et al.*, Phys. Rev. A **47**, 4517 (1993).
11. OBELIX Collaboration, M. Agnello *et al.*, Phys. Rev. Lett **74**, 371 (1995).
12. OBELIX Collaboration, A. Bertin *et al.*, Phys. Rev. A **54**, 5441 (1996).
13. P. Hauser, F. Kottmann, Ch. Lüchinger, R. Schaeren, in *Muonic Atoms and Molecules*, edited by C. Petitjean and L. Schaller (Birkhäuser, Basel 1993), p. 235.
14. W. Schott, H. Daniel, F.J. Hartmann, W. Neumann, Z. Phys. A **346**, 81 (1993).
15. H. Daniel, F.J. Hartmann, W. Neumann, W. Schott, Phys. Lett. A **191**, 155 (1994).
16. H.H. Andersen, J.F. Ziegler, *Hydrogen stopping powers and ranges in all elements* (Pergamon, New York 1977), Vol 3.
17. P.D. Fainstein, G.H. Olivera, R.D. Rivarola, Nucl. Instr. Methods B **107**, 19 (1996).
18. G. Schiwietz, U. Wille, R. Diez Muiño, P.D. Fainstein, P.L. Grande, J. Phys. B **29**, 307 (1996).
19. Yu. S. Sayasov, J. Plasma Physics **57**, 373 (1997).
20. P. Wojciechowski, P. Baumann, H. Daniel, F.J. Hartmann, M. Mühlbauer, W. Schott, A. Fuchs, P. Hauser, K. Lou, C. Petitjean, D. Taqqu, F. Kottmann, in *Muonic Atoms and Molecules*, edited by C. Petitjean, L. Schaller (Birkhäuser, Basel 1993), p. 345; P. Wojciechowski, Ph.D. thesis, Technische Universität München, 1995 (unpublished).
21. C. Varelas, J.P. Biersack, Nucl. Instr. Methods **79**, 213 (1970).
22. J.F. Janni, At. Data Nucl. Data Tables **27**, 147 (1982).
23. R. Golser, D. Semrad, Nucl. Instr. Methods B **69**, 18 (1992).
24. J.S. Cohen, Phys. Rev. A **27**, 167 (1983).
25. H.H. Mikkelsen, Nucl. Instr. Methods B **58**, 136 (1991).